Received: 24 October 2016 | Accepted: 8 January 2017

DOI: 10.1111/jace.14803

RAPID COMMUNICATION

Journal of the American Ceramic Society

Effect of metallic Ag growth on the electrical resistance of 3D flower-like $Ag_4V_2O_7$ crystals

Regiane C. de Oliveira[1] | Sonia M. Zanetti[2] | Marcelo Assis[1] | Maya Penha[1] | Mayara Mondego[1] | Mario Cilense[2] | Elson Longo[2] | Laécio S. Cavalcante[3]

[1]INCTMN-CDMF, Universidade Federal de São Carlos, São Carlos, SP, Brazil

[2]INCTMN-UNESP, Universidade Estadual Paulista, Araraquara, SP, Brazil

[3]PPGQ-CCN-DQ, Universidade Estadual do Piauí, Teresina, PI, Brazil

Correspondence
L.S. Cavalcante, PPGQ-CCN-DQ, Universidade Estadual do Piauí, Teresina, PI, Brazil.
Email: laeciosc@bol.com.br

Funding information
CAPES, Grant/Award Number: PNPD – 1268069; FAPESP, Grant/Award Number: 2013/07296-2, 2013/26671- 9; CNPq, Grant/Award Number: 304531/2013-8.

Abstract

In this communication, we report for the first time the nucleation and growth of metallic Ag nanoparticles on the surface of 3D flower-like $Ag_4V_2O_7$ crystals, induced by accelerated electron beam irradiation. The growth of metallic Ag on the surfaces of $Ag_4V_2O_7$ crystals were studied by transmission electron microscopy (TEM) and energy dispersive X-ray spectroscopy (EDXS). According to TEM images and EDXS analyses, exposure to the electron beam induces a reduction process and the growth of metallic Ag nanoparticles on the surface of $Ag_4V_2O_7$ crystals. Moreover, the inductively coupled plasma optical emission spectrometry measurements indicated an excess of Ag and V vacancies at $Ag_4V_2O_7$ lattice. Finally, it was observed that the electrical resistance varies considerably with the exposure time to electron beam irradiation.

KEYWORDS

$Ag_4V_2O_7$ crystals, electrical resistance, metallic Ag nanoparticles

1 | INTRODUCTION

Due to their physical and chemical properties, silver vanadium oxide (SVO) semiconductors have a wide range of applications, including in electrochromic devices, lithium batteries, catalysts, gas sensors, and electrical and optical devices.[1-3] The literature shows that their electronic properties can be improved by incorporating metallic Ag nanoparticles (NPs) on the surface. This is because the formation of a heterojunction creates a synergistic effect between Ag NPs and SVOs, improving their electronic properties.[4]

Recently, our group discovered a unwanted real-time in situ nucleation and growth processes of metallic Ag NPs on different silver-based semiconductors, such as α-Ag_2WO_4,[5] β-Ag_2MoO_4,[6-8] Ag_3PO_4,[9] and β-$AgVO_3$.[10] The nucleation and growth processes were driven, in all cases, by accelerated electron beam irradiation from an electron microscope under high *vacuum*. The reasons for this physicochemical phenomenon have been discussed in recent publications.[6,8-11]

Therefore, in this communication, we present new findings on the electrical resistance changes with the growth of metallic Ag NPs in the surface of the 3D flower-like $Ag_4V_2O_7$ crystals.

2 | EXPERIMENTAL PROCEDURE

The details related to synthesis, characterization, and setup for electrical measurements of 3D flower-like $Ag_4V_2O_7$ microcrystals are presented in Supplementary Information.

3 | RESULTS AND DISCUSSIONS

Figure 1 shows the XRD pattern of $Ag_4V_2O_7$ crystals no irradiated by electron beams.

All the diffraction peaks can be assigned to the orthorhombic structure (ICDS No. 38065, space group: *Pbca*).[12] The lack of other peaks demonstrates the high

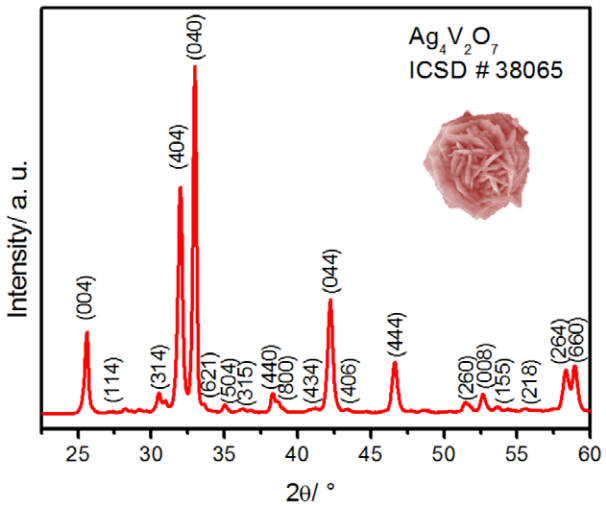

FIGURE 1 XRD patterns of 3D flowers-like $Ag_4V_2O_7$ microcrystals obtained at 0°C for 10 min [Color figure can be viewed at wileyonlinelibrary.com]

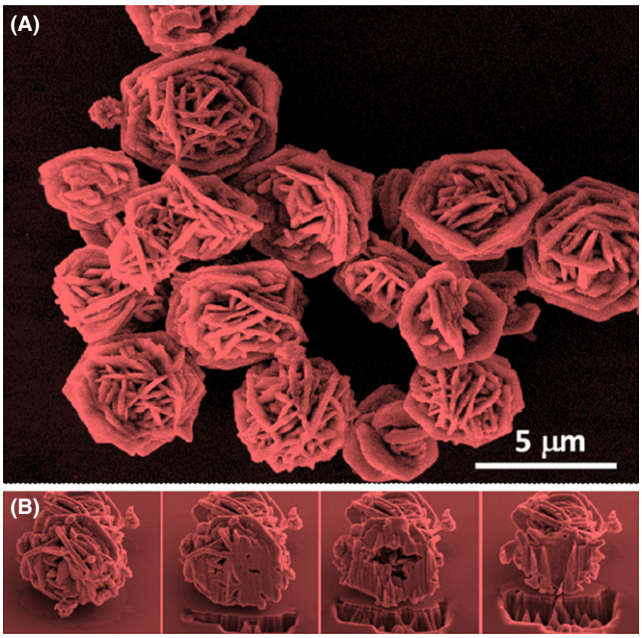

FIGURE 2 (A) Morphology and microstructure of the 3D flowers-like $Ag_4V_2O_7$ microcrystals and (B) Slicing of the 3D flowers-like $Ag_4V_2O_7$ microcrystals [Color figure can be viewed at wileyonlinelibrary.com]

purity of the materials. Detailed Rietveld refinement results are displayed in Figure S1 Supplementary Information (SI).

The morphology and microstructure of nonirradiated $Ag_4V_2O_7$ crystals were investigated by field-emission scanning electron microscopy (FE-SEM). In Figure 2A, can be seen that the $Ag_4V_2O_7$ crystals exhibit a uniform 3D flower and nearly spherical shape with an average diameter of 4.3 μm. The flower-like precursor is composed of very thin petals with an average thickness of approximately 170 nm.

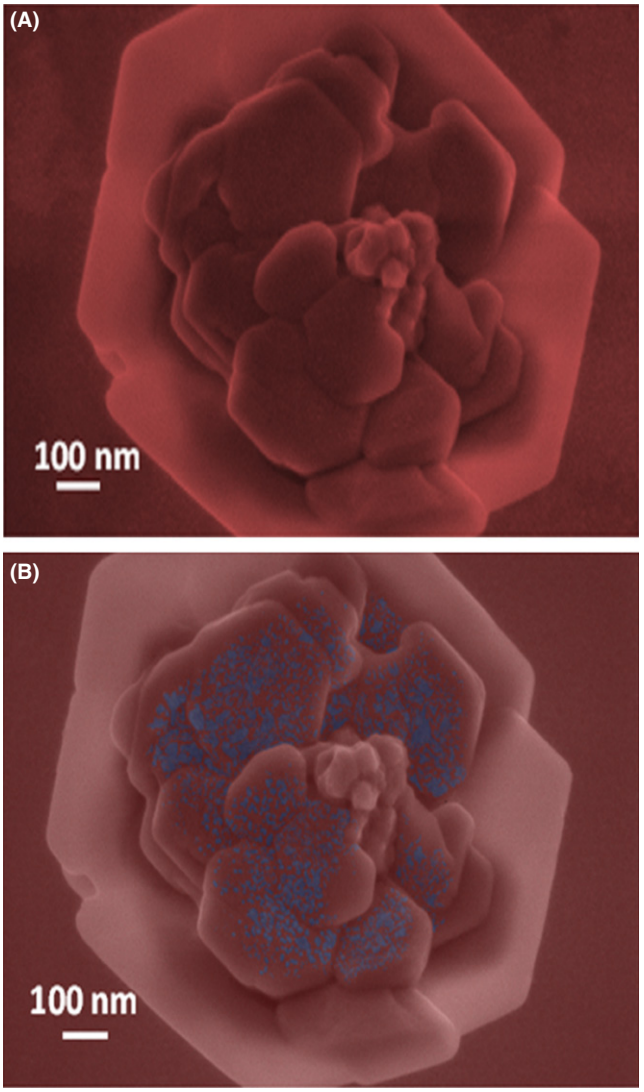

FIGURE 3 FE-SEM images of $Ag_4V_2O_7$ microcrystals: (A) before; and (B) after a 5 min exposure to the electron beam at 10 kV [Color figure can be viewed at wileyonlinelibrary.com]

Crystal size distributions were statistically analyzed by measuring 100 microcrystals from FE-SEM images (Figure S2 in Supporting Information). Only small variations in average particle sizes were observed, confirming the monodisperse nature of these particle systems.

A possible formation mechanism of the flower-like $Ag_4V_2O_7$ crystals could be described as follows: initially vanadium and silver complex clusters form in separate aqueous solutions. When the two solutions are mixed, $Ag_4V_2O_7$ nuclei clusters form and subsequently grow. The growth mechanism is governed by the Ostwald ripening process. The nanocrystals pass through a self-organization process and a few tiny nanoplates (NPLs), with some poorly defined hexagonal faces develop. Ten minutes after the reaction starts, undeveloped flower-like $Ag_4V_2O_7$ crystals start forming by self-assembly and preferential orientation process. Moreover, internal pores and channels were

observed when the flower-like crystals are sliced (Figure 2B). It is believed that these defects arise from the fast nucleation process, growth, and agglomeration onset of primary NPLs at a low temperature (0°C), which lead to the formation of relatively unordered flower-like crystals.

The growth process of metallic Ag NPs on the surface of $Ag_4V_2O_7$ crystals as a function of exposure time was investigated via FE-SEM under an accelerating voltage of 10 kV. The onset of Ag nanoparticle nucleation on the surface of the $Ag_4V_2O_7$ crystals was observed (Figure 3A,B) as soon as the sample analysis by FE-SEM image was started. Figure 3A shows an SEM image of the flower-like crystals immediately after a rapid approach and focus adjustment (time zero). After 5 minute of exposure to the electron beam, the $Ag_4V_2O_7$ crystals were already showing regions with Ag NPs on the surface, as can be seen in Figure 3B.

The EDXS and TEM analyses were used to prove that Ag NPs had grown on the surface of the $Ag_4V_2O_7$ crystals. The samples were subjected to electron beam irradiation in a TEM microscope for 2 minute, and two regions in the focused flower-like $Ag_4V_2O_7$ crystals were selected for examination. Figure 4A,B correspond to the sample before and after irradiation, respectively. In Figure 4B, two distinct regions (indicated in the figure by blue squares) were selected. In Region 1, Ag NPs were found and their presence was confirmed by EDXS analysis. The EDXS results (Figure 4B, Region 1) confirmed that the electron beam promoted the random growth of metallic Ag NPs. The material in Region 2 was composed of Ag, V, and O. The inductively coupled plasma optical emission spectrometry (ICP-OES) measurements are presented in Table S1 and shown in (Supporting Information) indicated an excess of Ag and V vacancies at $Ag_4V_2O_7$ lattice.

To the best of our knowledge, this phenomenon had not been previously observed for $Ag_4V_2O_7$ and was found to occur in all regions irradiated by the electron beam. A complex clusters model based on Kröger-Vink[13] notation was employed to further explain the electrical properties of $Ag_4V_2O_7$ crystals and propose a possible electrical resistance observed at system. In this model, intrinsic (bulk/surface) defects in the lattice of the material facilitate polarization of the lattice and lead to the electronics transitions between ordered and disordered clusters. Therefore, electron (e')-hole ($h^{\bullet}$) pairs are present even before excitation of lattice. The before and after exposure to electron beam enhances the formation of e'-$h^{\bullet}$ pairs leading to electron transfer within the band gap. The cluster-to-cluster charge-transfer (CCCT) in a crystal, containing more than one kind of cluster,[14] is characterized by excitations involving electronic transitions from one cluster to another, which is possible according to Equations (1-6):

$$\xrightarrow{e'}[Ag_4V_2O_7]_{(defects)} \rightarrow 4Ag_i^{\cdot} + 2V_V^{2'} + 7O_O^x \quad (1)$$

$$\xrightarrow{e'}[Ag_4V_2O_7]_{(defects)} \rightarrow [AgO_6]_o^x - [AgO_6]_d^x + [AgO_5]_o^x - [AgO_5]_d^x + [VO_5]_o^x - [VO_5]_d^x + [VO_4]_o^x - [VO_4]_d^x \quad (2)$$

$$[AgO_6]_o^x - [AgO_6]_d^x \xrightarrow{e'} [AgO_6]_o' - [AgO_6]_d^{\bullet} \quad (3)$$

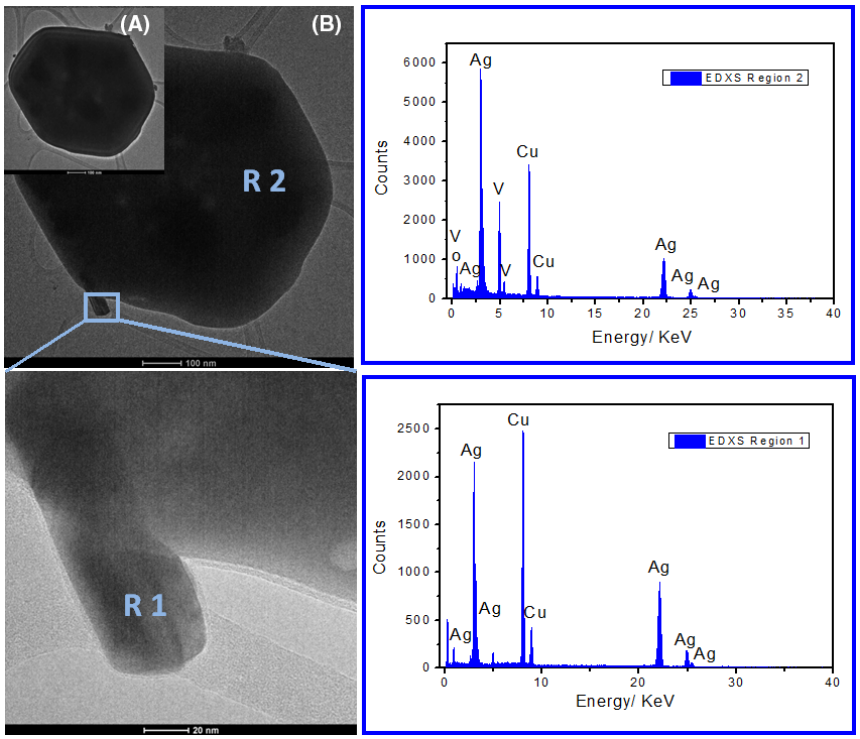

FIGURE 4 TEM images of $Ag_4V_2O_7$ microcrystals: (A) before; and (B) after a 5 min exposure to the electron beam at 10 kV [Color figure can be viewed at wileyonlinelibrary.com]

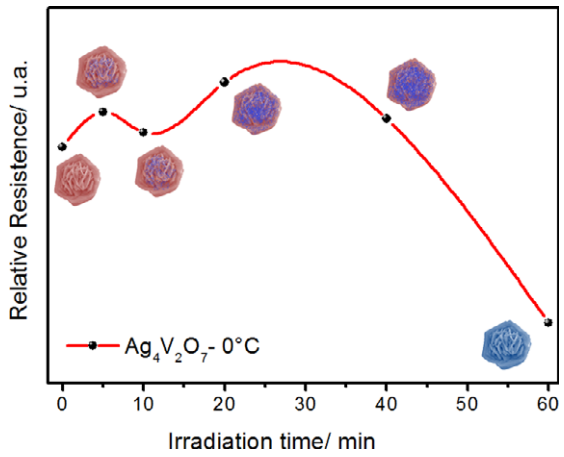

FIGURE 5 Variation in the electric resistance of $Ag_4V_2O_7$ microcrystals subjected to electron beam irradiation for different times [Color figure can be viewed at wileyonlinelibrary.com]

$$[AgO_5]_o^x - [AgO_6]_d^x \xrightarrow{e'} [AgO_6]_o' - [AgO_6]_d^{\bullet} \quad (4)$$

$$[VO_5]_o^x - [VO_5]_d^x \xrightarrow{e'} [VO_5]_o' - [VO_5]_d^{\bullet} \quad (5)$$

$$[VO_4]_o^x - [VO_5]_d^x \xrightarrow{e'} [VO_4]_o' - [VO_4]_d^{\bullet} \quad (6)$$

When the surface of 3D flower-like $Ag_4V_2O_7$ crystals is irradiated with an electron beam, the lattice composed by ordered(o)/disordered(d) $[AgO_5]/[AgO_5]$ and o/d $[VO_5]/[VO_4]$ clusters interact with the incoming electrons, resulting in the reduction process of Ag NPs, formation of excess Ag and interstitial Ag ($Ag_i^{\cdot}$), as well as the formation of V vacancies ($V_V^{2'}$). Moreover, Ag migrates from the bulk to the surface; hence, regions in the crystal lattice with negatively charged vacancies form. This process induces a short- and medium-range disorder within the material. The regions where the metallic Ag has migrated exhibit a *p*-type semiconducting behavior. Since $Ag_4V_2O_7$ crystal is an *n*-type semiconductor and oxygen vacancies ($V_O^{\bullet}$) are already present, an *n*/*p* interface is created between the Ag NPs and $Ag_4V_2O_7$ crystals, thereby forming a semiconductor diode. A semiconductor diode has the valuable property that electrons only flow in one direction across it, and as a result, it acts as a rectifier.[10]

Since the Ag growth on flower-like $Ag_4V_2O_7$ crystals can affect the electrical properties of the material, electrical resistance measurements were performed, and the results were evaluated as a function of the exposure time, ie, as a function of the growth of these metallic Ag nanoparticles. Figure 5 shows the variation in the electrical resistance of flower-like $Ag_4V_2O_7$ crystals subjected to electron beam irradiation at different exposure times.

Before the formation of Ag NPs, the electrical resistance is governed by the bulk properties, the shape of the crystals, and the presence of pores and channels in the bulk. After 5 minute irradiation, a slight increase in resistance is observed, which can be attributed to the pores and channels in the bulk. From this time until 10 minute, the bulk and surface properties equally contribute to the semiconductor resistance. After 10 minute, the growth of Ag NPs silver on the $Ag_4V_2O_7$ surface creates Ag vacancies (V'_{Ag}), $Ag_i^{\cdot}$ and $V_V^{2'}$ in the semiconductor bulk (Equation 1). The formation of negative V'_{Ag}, along with the already present oxygen vacancies ($V_O^{\bullet}$), causes an increase in the electrical resistance of the semiconductor, until the irradiation time reaches 27 minute. However, after 27 minute, the resistance decreases, probably due to the formation of a thick layer of metallic Ag on the $Ag_4V_2O_7$ semiconductor surface, which continues to grow with the irradiation time. Since the Ag is the best-known electric conductor (room temperature), this growth of the Ag metallic layer acts decreasing the electrical resistance of the material.

4 | CONCLUSION

In summary, we have observed, for the first time, that electron beam irradiation, such as that produced by FE-SEM/TEM, induces the formation and growth of metallic Ag NPs on the surface of 3D flower-like $Ag_4V_2O_7$ crystals. ICP-OES measurements showed the presence of V vacancies and excess of Ag at $Ag_4V_2O_7$ lattice. Moreover, it was observed that the electrical resistance of the flower-like $Ag_4V_2O_7$ crystals is largely influenced by the growth of Ag NPs on the surface of the semiconductor. Therefore, the irradiation-generated Ag NPs have two advantageous effects: the formation of Ag NPs on the crystal surface and control of the semiconductor properties by electron beam irradiation.

ACKNOWLEDGMENTS

The authors acknowledge the financial support of agencies: CAPES (PNPD – 1268069), FAPESP (2013/07296-2; 2013/26671- 9), and CNPq (304531/2013-8).

REFERENCES

1. Ran R, McEvoy JG, Zhang Z. $Ag_2O/Ag_3VO_4/Ag_4V_2O_7$ heterogeneous photocatalyst prepared by a facile hydrothermal synthesis with enhanced photocatalytic performance under visible light irradiation. *Mater Res Bull*. 2016;74:140-150.
2. Zeng H, Wang Q, Rao Y. Ultrafine β-$AgVO_3$ nanoribbons derived from α-$AgVO_3$ nanorods by water evaporation method and its application for lithium ion batteries. *RSC Adv*. 2015;5:3011-3015.
3. Sharma S, Panthöfer M, Jansen M, Ramanan A. Ion exchange synthesis of silver vanadates from organically templated layered vanadates. *Mater Chem Phys*. 2005;91:257-260.
4. Zhao W, Guo Y, Faiz Y, et al. Facile in-suit synthesis of Ag/$AgVO_3$ one-dimensional hybrid nanoribbons with enhanced

performance of plasmonic visible-light photocatalysis. *Appl Catal B: Environm*. 2015;163:288-297.
5. Longo E, Cavalcante LS, Volanti DP, et al. Direct in situ observation of the electron-drivensynthesis of Ag filaments on α-Ag_2WO_4 crystals. *Sci Rep*. 2013;3:1676-1680.
6. Alvarez Roca R, Lemos PS, Andrés J, Longo E. Formation of Ag nanoparticles on metastable β-Ag_2WO_4 microcrystals induced by electron irradiation. *Chem Phys Lett*. 2016;644:68-72.
7. De Santana YVB, Gomes JEC, Matos L, et al. Silver molybdate and silver tungstate nanocomposites with enhanced photoluminescence. *Nanomater Nanotechnol*. 2014;4:22-31.
8. Andrès J, Ferrer MM, Gracia L, et al. A combined experimental and theoretical study on the formation of Ag filaments on b-Ag2MoO4 induced by electron irradiation. *Part Part Syst Char*. 2015;32:646-651.
9. Botelho G, Sczancoski JC, Andres J, Gracia L, Longo E. Experimental and theoretical study on the structure, optical properties, and growth of metallic silver nanostructures in Ag_3PO_4. *J Phys Chem C*. 2015;119:6293-6306.
10. Oliveira RC, Assis M, Teixeira MM, et al. An experimental and computational study of ß-$AgVO_3$: optical properties and formation of Ag nanoparticles. *J Phys Chem C*. 2016;120:12254-12264.
11. Fabbro MT, Gracia L, Silva GS, et al. Understanding the formation and growth of Ag nanoparticles on silver chromate induced by electron irradiation in electron microscope: a combined experimental and theoretical study. *J Solid State Chem*. 2016;239:220-227.
12. Masse R, Averbuch-Pouchot MT, Durif A, Guitel JC. Chemical preparation and crystal structure of silver pyrovanadate, $Ag_4V_2O_7$. *Act Cryst*. 1983;C39:1608-1610.
13. Kröger FA, Vink HJ. *Relations Between the Concentrations of Imperfections in Crystalline Solids*. Solid State Phys. 3rd edn. Amsterdam, the Netherland: Elsevier; 1956.
14. Oliveira RC, Gracia L, Assis M, et al. Disclosing the electronic structure and optical properties of Ag4V2O7 crystals: experimental and theoretical insights. *Cryst Eng Comm*. 2016;18:6483-6491.

SUPPORTING INFORMATION

Additional Supporting Information may be found online in the supporting information tab for this article.

How to cite this article: de Oliveira RC, Zanetti SM, Assis M, et al. Effect of metallic Ag growth on the electrical resistance of 3D flower-like $Ag_4V_2O_7$ crystals. *J Am Ceram Soc*. 2017;100:2358–2362.